

UNIVERSITÀ DEGLI STUDI DI TORINO

SCUOLA DI SCIENZE DELLA NATURA

Corso di Laurea Magistrale in Fisica



Tesi di Laurea Magistrale

**TESTING OF THE TD26 TYPE  
CAVITY UNDER BEAM LOADING  
FOR THE CLIC PROJECT**

Relatore:

Prof. Martino Gagliardi

Co-relatore:

Dr. Frank Tecker (CERN)

Candidato:  
Eugenio Senes

Controrelatore:

Prof. Ferruccio Balestra

Anno Accademico 2015/2016

Considerate la vostra semenza:  
fatti non foste a viver come bruti,  
ma per seguir virtute e canoscenza

Dante, *La Divina Commedia*  
Canto XXVI

# Abstract

*(Leave this for the moment ....)*

A new generation of colliders capable of reaching TeV energies is under development nowadays, and to succeed in this task is necessary to show that the technology for such machine is available. The CLIC project is one of the most advanced design among the possible lepton colliders, and is formed by two normal conducting LINACs. To reach such high energies are necessary accelerating structures carrying gradient beyond 100MV/m and one of the biggest limitations is developing accelerating structures that present a sufficient low occurrence of vacuum arcs. This is pursued both with the design and the *conditioning*, which is the process of increasing the resilience to vacuum arcs of a structure using repetitive RF pulsing sessions.

The focus of this work is on the breakdown rate testing of the TD26 type cavity with and without beam presence inside. At CERN this test has been carried out on the cavity installed in the *dogleg* line in the CLIC-test-facility 3 (CTF3), and connected on the RF side to the X-band test stand 1 (Xbox1).

Other peculiar properties of the operation have been studied also, such has beam-induced RF generation into the cavity after the breakdowns, breakdown migration, ....

# Italian abstract

*(Translate once you have the ok to the english one)*

# Contents

<b>1</b>	<b>Introduction</b>	<b>1</b>
1.1	Generalities on colliders . . . . .	2
1.2	The CLIC project and the CTF3 facility . . . . .	4
1.2.1	Physics and staging . . . . .	5
1.2.2	Main parameters and main issues . . . . .	7
1.2.3	CTF3 . . . . .	8
<b>2</b>	<b>Accelerating structures</b>	<b>9</b>
2.1	Travelling wave accelerating structures . . . . .	9
2.1.1	Synchronous particle acceleration . . . . .	9
2.1.2	Reminder of Electromagnetism . . . . .	10
2.1.3	Periodic accelerating structures . . . . .	11
2.1.4	Figure of merit for accelerating structures . . . . .	13
2.2	High power limits and scaling laws . . . . .	14
2.2.1	Field emission law . . . . .	15
2.2.2	Kilpatrick's critereon . . . . .	16
2.2.3	Power flow based criteria . . . . .	18
2.2.4	The modified Poynting vector $S_c$ . . . . .	18
2.3	The TD26CC structure for the Main Beam of CLIC . . . . .	20
<b>3</b>	<b>The breakdown process</b>	<b>23</b>
3.1	phase1 . . . . .	23
3.2	phase2 . . . . .	23
3.3	phase3 . . . . .	23
<b>4</b>	<b>Experimental setup</b>	<b>24</b>
4.1	Main beam accelerating structure . . . . .	24
4.2	Linac and dogleg . . . . .	24
4.3	RF power generation . . . . .	24
4.4	DAQ system . . . . .	25
4.4.1	Hardware . . . . .	25
4.4.2	Online triggers . . . . .	25
4.5	Other systems . . . . .	25

## CONTENTS

---

<b>5 Data analysis tools</b>	<b>26</b>
5.1 Offline selection of the events . . . . .	26
5.2 Time and space positioning of the breakdowns . . . . .	26
5.3 Migration of the breakdowns . . . . .	26
5.4 Beam induced RF . . . . .	26
5.5 Neural network based events selection . . . . .	26
<b>6 Results and future developments</b>	<b>27</b>
6.1 Results . . . . .	27
6.2 Further developments . . . . .	27
<b>List of abbreviations</b>	<b>28</b>
<b>Bibliography</b>	<b>31</b>

# Chapter 1

## Introduction

Particle accelerators occupy a key role both in fundamental research and in all the applications and industrial processes that uses technology and processes developed initially for the elementary research.

A number of examples could be named among the spin-offs of accelerators' science, the most notable nowadays is the enormous progress of nanosciences in the last decade, that was made possible by the availability of high-brilliance light sources provided by synchrotrons, that was achievable thanks to the experience developed in the production of high quality electron beams. In the same way to inquire a much smaller scale are necessities machines involving greater energies, and the development of the latter will lead the one of the former and so forth. Hence in this perspective keep developing the accelerators for the physical research is a fundamental requirement to assure that the cutting-edge technology of today turns into the "labware" of tomorrow for all the other sciences and the industry, in addition of the contribution that pursuing the fundamental research can give to our understanding of the world of the elementary particles.

Going back to the particle scale, at the moment the most successful model to explain the behaviour of the elementary particles is the *Standard Model*, but it's not conclusive and not able to answer to all the questions still open in particle Physics. A milestone in favour of the Standard Model was the observation of the Higgs Boson in 2012 [1, 2], and was made possible by the construction of the *Large Hadron Collider* at CERN[3]. However the full understanding of the physics at the particle scale still needs to be achieved. Partially this will be realised with the increase of the collision energy of the LHC, but also the International Committee for Future Accelerators (ICFA) consider that the results of LHC needs to be complemented by the results of a lepton collider in the TeV-range[4].

The reason of this decision is that according to the standard model the hadrons are particles composed by quarks, that are continuously interacting exchanging gluons. This peculiarity cause the collision at high energy not to be between the hadrons themselves, but between partons composing them. In addition, there is no way to know in advance the energy of the partons

involved, so it's not possible to know in advance which will be the energy of the collision. For example it is improbable for a parton in the 14 TeV centre-of-mass energy LHC to have much more than 1-2 TeV of energy at the interaction point[5]. On the other hand, the leptons are punctual particles, so the interaction is directly involving the two bullets themselves at a given energy, and the number of possible processes that can take place is definitely smaller.

This key difference in the behaviour of leptons and hadrons makes hadron colliders *machines for discovery*, because involve all the possible processes that can take place in a wide range of energies, and the lepton machines *machines for precision*, because the reduced number of possible processes guarantees the observation of the events of interest much easier.

## 1.1 Generalities on colliders

According to the beam use two kinds of accelerators can be distinguished:

1. Fixed target: where a beam is shoot against a non-moving target. The energy in the centre-of-mass is  $E_{CM} = \sqrt{E_{BEAM}}$
2. Colliders: where two beams are accelerated in opposite directions and then made collide on each other. In this case the energy of the centre-of-mass is  $E_{CM} = E_{BEAM1} + E_{BEAM2}$

therefore is easy to see that to reach a high centre-of-mass energy the collider topology is preferable.

Once the collision have taken place and got revealed, the rate of observation of a particular interaction process A is given by

$$\frac{dN(A)}{dt} = \mathcal{L} \sigma(A) \quad (1.1)$$

where  $\sigma$  is the process cross-section, which depends by the physics of the process A itself, and  $\mathcal{L}$  is the luminosity, which depends entirely by the machine. Therefore the figure of merit when it comes to talk about accelerators is the luminosity, which is given by

$$\mathcal{L} = H_d \frac{N^2}{\sigma_x \sigma_y} n_b f_r \quad (1.2)$$

where  $N$  is the number of particles per bunch,  $\sigma_x$  and  $\sigma_y$  are the beam dimensions in the horizontal and vertical plane,  $n_b$  is the number of particle per bunch,  $f_r$  is the collision frequency of the bunches and  $H_d$  is a correction factor that takes in account the non ideality of the collision, such as crossing angle, collision offset, hour glass effect, non gaussian beam profile and so on.

Then becomes necessary try to reach the highest luminosity possible since the events that are going to be studied are rare. This is realised differently according to the design of the accelerating machine in use:

- linear accelerators (LINACs): present a low repetition frequency, typically lower than hundred of Hz and the beam is passing just once to be accelerated through the machine.
- circular accelerators (typically synchrotrons): have a higher repetition frequency, up to tenth of KHz, and are keeping the particle beam in orbit for many turns, so can accelerate it over a long period of time

After this distinction one could be led to think that the circular machine is the best choice in any case in order to reach high luminosity, but raising the energy of the beam a big issue comes out: the power loss in circular machines due to the emission of synchrotron radiation scales according to the following expression

$$P \propto \frac{1}{\rho^2} \frac{E^4}{m_0^4} \quad (1.3)$$

where  $\rho$  is the bending radius of the machine,  $E$  is the particle energy and  $m_0$  is its rest mass. As can be noted in the table 1.1, the energy loss per turn is a relevant fraction of the beam energy, e.g. for the LEP machine over than 3 GeV were lost per turn, while the record energy per beam was 104.5 GeV. To raise the beam energy and reduce the energy loss, the radius of circular machines escalates quickly. Simply scaling LEP, it is possible to show that in order to reach the centre-of-mass energy of 3 TeV, the circumference should be increased to thousands of kilometers [6]. To solve the issue the development of new lepton colliders is so focusing on two different solutions:

1. Use muons instead of electrons: this innovative approach reduces the power lost because of the higher mass of the muon compared to the electron, but has to deal with the short life of muons, which is roughly  $2 \mu s$  in the laboratory frame
2. Limit the losses caused by synchrotron radiation, or increasing the bending radius or abandon the circular topology for the linear one

Also has to be noted that the former technology is rather new and needs to still be fully developed, while the latter profits of the progresses achieved in the last half century mainly in SLAC and KEK on the LINAC technology.

In this perspective a number of project are under study at the moment, of wich the most ambitious are FCC-ee, *Future Circular Collider*, ILC, *International Linear Collider*, and CLIC, *Compact Linear Collider*. The first one consist in a circular collider which is supposed to be placed in a 80-100 km long tunnel before of the installation of the FCC-hh, the other are LINACs even if based on completely different technologies and solutions. A comparison of the features of these projects in the final stage is presented in the table 1.1, and also LEP is presented as example of circular lepton collider.

Furthermore a recent interest arose on more compact technologies, e.g. plasma acceleration techniques, but the reliability of such designs still need to be proven in the perspective of creating a fully functional machine that goes beyond the demonstration of the working physical principle.

Parameter	LEP2	FCC-ee	CLIC		ILC
$\sqrt{s} [GeV]$	209	350	500	3000	500
$\mathcal{L}_{peak} [10^{34} cm^{-2} s^{-1}]$	0.012	1.3	2.3	5.9	1.8
Total lenght [km]	26.7	100	13	48.4	31
$E_{acc}^{loaded} [MV/m]$		10 - 20	80	100	31.5
Bunch population [ $10^9$ ]	105	170	6.8	3.72	500
Bunch spacing [ns]		4000	0.5	0.5	554
Collision rate [Hz]		$\approx 3000$	50	50	5
$\epsilon_x^* / \epsilon_y^* [\mu m] / [nm]$		0.68/0.68	2.4/25	0.66/20	10/35
$\sigma_x^* / \sigma_y^* [nm]$		3600/70	202/2.3	40/1	474/5.9
Energy loss [GeV turn $^{-1}$ ]	3.34	7.55	-	-	-
AC Power [MW]		$\approx 300$	271	582	163

Table 1.1: Comparison of two circular machines, LEP[7] and FCC-ee[7, 8] and the two projects for linear machines, the fist and last stage of the CLIC implementation [9] and the final stage of ILC[10]

## 1.2 The CLIC project and the CTF3 facility

The *Compact Linear Collider* is the project for a linear electron-positron collider capable of reaching a centre-of-mass collision energy of 3 TeV and a luminosity of  $2 \times 10^{34} cm^{-2} s^{-1}$  in the final stage.

The realisation of such machine implies many technological challenges in order to keep the power consumption and the dimension limited while matching the design goal parameters. These challenges have been faced developing the novel *two-beam acceleration scheme*, in which the idea is to use a high-current and low-energy beam, the *Drive Beam*, in order to generate the RF power to accelerate a low-current and high-energy beam used for the experiments, named *Main Beam*.

The Drive Beam is produced using a dedicated LINAC, and then the current is multiplied using a delay loop and two recombination rings, reaching a combination factor of  $2 \times 3 \times 4 = 24$ . This topology generates the beam with a final frequency of the bunches of 12 GHz, and the reason for this kind of implementation is to reach the highest possible efficiency in the Drive Beam production, in order to shrink the power consumption to the smallest possible. To reach this goal the acceleration in the LINAC is performed using the accelerating cavities in fully-loaded mode.

While the biggest challenge for the main beam is reaching the necessary high current, for the Main Beam the hardest challenge is generating a beam with the smallest dimension possible, in order to increase the luminosity of the machine as much as possible.

The Main Beam is produced in a separate facility, where a DC-photo gun system provides the initial polarised electron beam, and afterwards part of the beam is sent to a target in order to generate the positron beam. Once both the beams have been produced, they are sent to the next accelerating stages,

which are composed of LINACs to raise the beam's energy and of damping rings to reduce the emittances.

The detailed description of the Main Beam production and the Drive Beam recombination process can be found in [9] and about how the working principle have been demonstrated in the CTF3 in [11].

Once both beams have been produced, are sent to the common tunnel where the Two-beams modules are installed. The Two-beam module is composed by two principal sections, which are the PETS, *Power Extraction and Transfer Structures*, and the accelerating structures for the Main Beam, as exploited in figure 1.2. The Main Beam passes through the PETS and gets decelerated. As product of the deceleration a pulse of RF power is produced, which is transferred by a waveguide network and used to accelerate the Main Beam. In this way it is possible to reach an efficient acceleration of the Main Beam up to the desired energy for the experiments

### 1.2.1 Physics and staging

The machine is designed to be built in 3 stages, with a final energy of 3 TeV.

Since the CDR[9] was released just before the discovery of the Higgs boson, the centre of mass energy stages have been reshaped in order to be able to access to interesting measurements, anyway for a given centre-of-mass energy, the energy can be modified by a third with limited loss of performance[12], allowing an eventual retuning of the energy of the stages following the results of the last LHC physics campaign.

The energy staging have been chosen as follows, further informations can be found in[13, 14], but the leading idea is to make accessible the Higgs and top physics from the first stage.

The first stage is proposed to be 380 GeV, and it gives access to the Standard model Higgs physics and top-quark physics. The measurements on the former can be conducted through Higgsstrahlung and WW-fusion processes, thereby providing accurate model-indipendent measurements of Higgs couplings to bosons and fermions[15]; the latter measurements will be focused on the  $t\bar{t}$  pair production threshold in the vicinity of  $\sqrt{s} = 350$  GeV.

The second stage is proposed at 1.5 TeV and allows to access new physics phenomena and additional properties of the Higgs boson and the top quark, such as Higgs self-coupling and rare Higgs branching ratios.

The third stage is proposed at 3 TeV and will give direct access to pair-produced particles with mass up to 1.5 TeV or single particles with mass up to 3 TeV. This stage is particularly interesting as test for the BSM theories, since such high energy in a lepton machine makes the observation of new particles much easier than in the LHC.

A further remodulation of these steps is possible after the publication of the results of the run 2 of the LHC, but anyway the advantage of a linear machine in this sense is that the final energy can be reshaped modifying the total length of the machine. In figure 1.3 is shown the track of a possible CLIC

## CHAPTER 1. INTRODUCTION

---

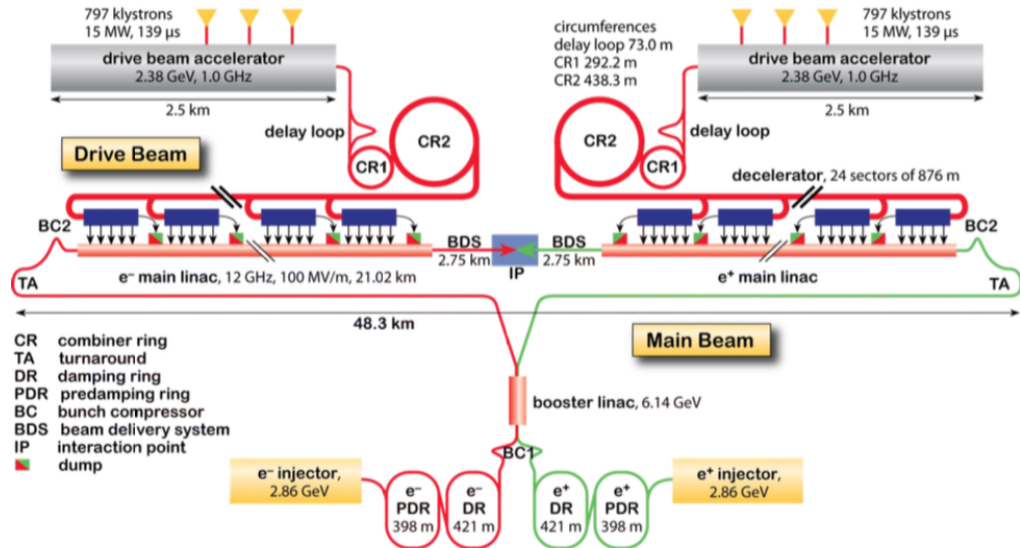


Figure 1.1: Layout of the final stage of CLIC

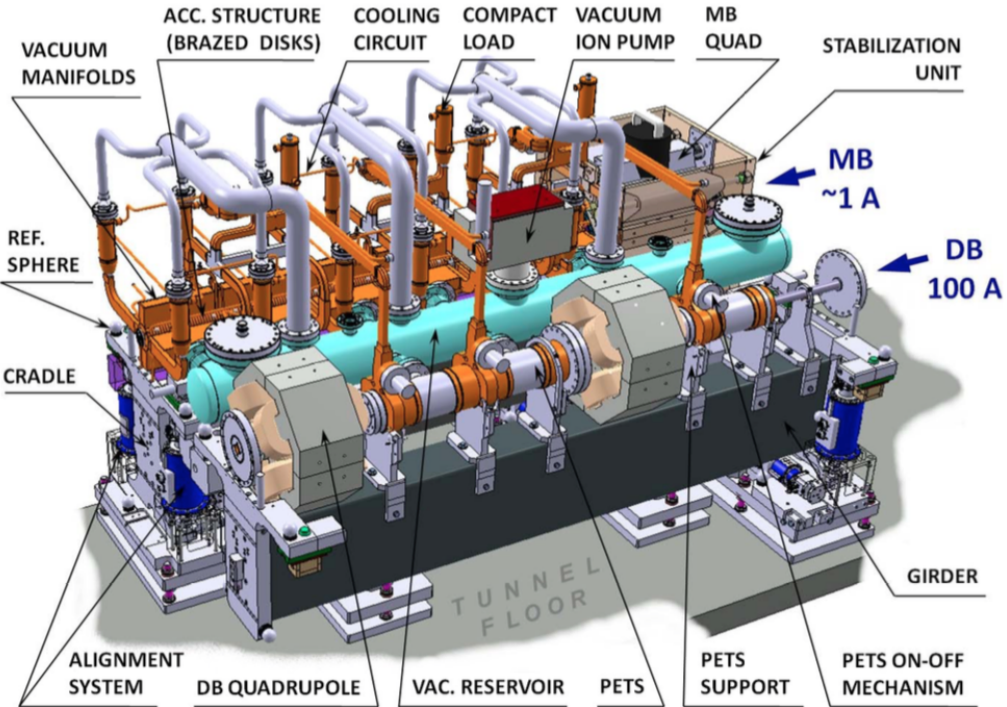


Figure 1.2: Design of a Two-beam module.

build in the Geneva area, in order to give an idea about the order of magnitude of that kind of facility compared to LHC and SPS.

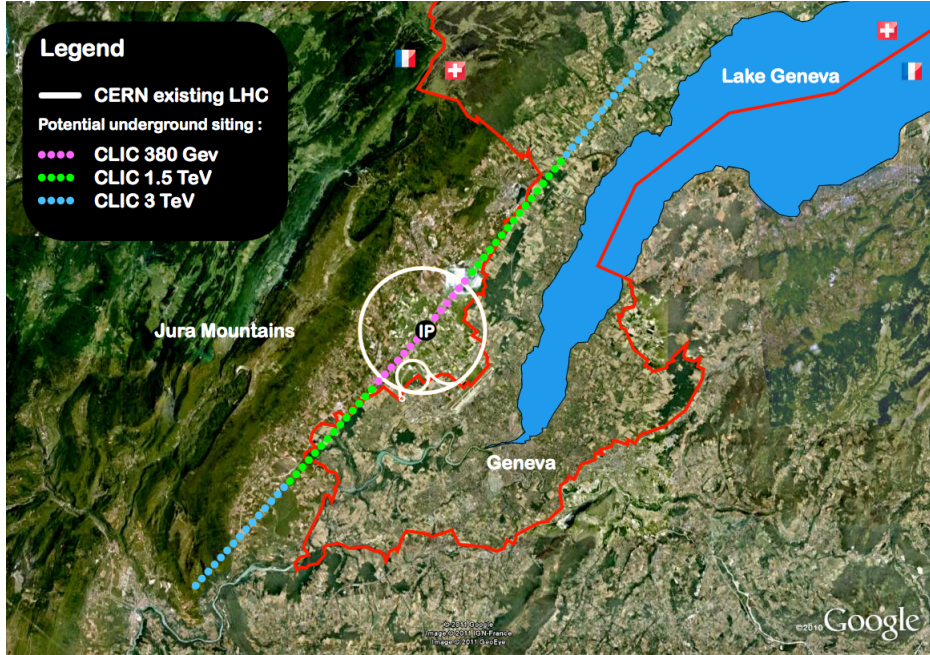


Figure 1.3: Map of the CLIC facility, if implemented in the Geneva area

### 1.2.2 Main parameters and main issues

There are many issues that can affect the performance of a machine like CLIC, and need to be analysed carefully since no similar machine have been built so far. The main issues are:

1. 100 MV/m accelerating gradient: this requirement comes from the final energy of 3 TeV and the requirement of a maximum length of 50 km
2. Breakdown rate  $< 3 \times 10^{-7}$  breakdowns per pulse per meter: this limitation comes from the limit on design luminosity loss in case of breakdown. Is the aim of this work and will be stressed in detail later
3. Transverse wakefields limitation: wakefields have to be considered because of the short bunch spacing in the bunch train. If not limited are a serious issue to the luminosity.
4. Powering the accelerating structures: no klystrons on the market are able to produce high power pulses 150-200 ns long. This requires the use of pulse compression systems or the two-beam acceleration scheme, that have never built and operated so far in a functional collider
5. Generate the drive beam with an efficiency of 97% in order to contain the power consumption. Also the efficiency of the power transfer between the beams is a key issue in order to reach the energy goal

6. Extremely small beam emittance and size: in order to match the luminosity goal with the typical low repetition rate of a LINAC is necessary to squeeze the beam as much as possible, reaching the goal of 40 and 1 nm at the interaction point in the horizontal and vertical plane. This parameter includes the realisation of a nanometric alignment and vibration containing system

Therefore the parameters in the table 1.2 have been selected in order to match the design parameters reported in the table 1.1 for the top design energy.

Description	CLIC 3 TeV
Peak luminosity [ $cm^{-2}s^{-1}$ ]	2.0x10 <sup>34</sup>
Total site length [km]	48.4
Loaded accelerating gradient [MV/m]	100
Main LINAC RF frequency [GHz]	12
Charge per bunch [nC]	3.7x10 <sup>9</sup>
Bunch separation [ns]	0.5
Bunches per train	312
Beam pulse duration [ns]	156
$\epsilon_x^* / \epsilon_y^*$ [ $\mu m$ ]/[nm]	0.66/20
$\sigma_x^* / \sigma_y^*$ [nm]	40/1

Table 1.2: CLIC main parameters in the final stage

### 1.2.3 The CLIC Test Facility 3

To be able to assert that the CLIC scheme is a feasible and reliable technology to build a functional collider, a number of tests have to be conducted since no accelerators using the Two-beam acceleration concept have been reached the production phase yet. To satisfy this requirement at CERN have been realised the CLIC Test Facility, that is in charge of demonstrate experimentally:

- The feasibility of the Drive Beam generation with a frequency of 12 GHz, performing the beam recombination using a delay loop and a combiner ring for a total multiplication factor of  $2 \times 4 = 8$
- The RF power production using the PETS and investigate the possible issues of the Two-beam scheme

In addition a branch of the LINAC was used to perform high-gradient tests with the beam presence inside the accelerating cavity, which is the topic of the following work.

# Chapter 2

## Accelerating structures

The accelerating structures are one of the key part of a particle accelerator. Even though in the first accelerators the particle acceleration was achieved simply with fixed fields, this technique showed its limitations quite soon due to the impossibility to create arbitrary high DC voltages without incur in electrostatic discharges. The present conventional technology for particle acceleration is based on the RF cavities, so it is natural try to push the state-of-the-art technology the further possible in order to reach the highest acceleration possible in the shortest length. In the case of the CLIC project a key issue is to be able to produce cavities with an accelerating field of 100 MV/m, which is the cutting-edge value at the moment when keeping the breakdown rate limited.

In this chapter some topics about the theory of accelerating cavities will be presented, the aim is to give to the reader a theoretical introduction to be able to understand the description of the cavity under test at the end of the chapter.

### 2.1 Travelling wave accelerating structures

In this section some useful concepts and result of the electromagnetic theory will be recalled. Because of conciseness, the examples and the geometries presented will refer to the travelling wave accelerating structures, since is the only type of structure relevant for the successive development of this work. The curious reader can find details on the untreated topics in [16, 17, 18] and in plenty of specialised books.

#### 2.1.1 Synchronous particle acceleration

A particle injected in an electromagnetic field in some conditions can gain energy at expenses of the field, getting accelerated. This is possible if the particle is injected at the right moment and the field and the particle have the same speed. In this manner the particle can travel with the field with an energy gain given by

$$\Delta W = qV_o \cos\phi \quad (2.1)$$

where  $q$  is the charge of the particle,  $V_0$  is the accelerating field and  $\phi$  is the relative phase between particle and RF field.

In order to deliver a constant energy gain to a charged particle it is necessary to shape the EM field matching two fundamental conditions:

1. The electromagnetic wave has to have a non-zero component in the direction of the motion of the particle
2. The phase velocity of a wave has to be the same of the particle velocity, in order to keep the relative phase constant, and so the acceleration

using some results of the theory of EM waves it is possible to show that the two condition cannot be met in the free space, but is necessary to build up some particular structures in order to coerce the electromagnetic field to propagate in the desired form. This is realised building particular structures that are similar to traditional waveguides, but presenting a lower phase velocity in order to make the synchronous acceleration possible.

### 2.1.2 Reminder of Electromagnetism

#### Maxwell's equations

It's well known since the basic courses of physics that the propagation of the electromagnetic fields follow the Maxwell's equations, that in a medium are

$$\begin{aligned} \nabla \cdot \vec{D} &= \rho_{free} \\ \nabla \cdot \vec{B} &= 0 \\ \nabla \times \vec{E} &= -\frac{\partial \vec{B}}{\partial t} \\ \nabla \times \vec{H} &= \vec{J}_{cond} + \frac{\partial \vec{D}}{\partial t} \end{aligned} \quad (2.2)$$

where  $\vec{E}$  and  $\vec{B}$  are the electric and magnetic field in the vacuum,  $\vec{D} = \epsilon \vec{E}$ ,  $\vec{B} = \mu \vec{H}$  and  $\vec{E} = \sigma \vec{J}$ . The propagation in vacuum is described by the same equations and can be easily derived with an appropriate choice of the constants.

#### Waveguides and resonant cavities

In some particular cases the confined propagation of electromagnetic waves is possible, and is commonly realised using a metal waveguide to direct all the energy in a single direction. In this section some useful results on the propagation in a waveguide will be stressed, the full derivation can be found in literature [19, 20, 16].

The request of propagation in the direction of the axis of the waveguide can be traduced to the condition  $\vec{E} \times \vec{n} = 0$ , that means asking that no power is dissipated in the walls of the cavity by Joule effect since the electric field is normal to the surface anywhere and anytime.

Many solutions can be found to the problem, integrating the Maxwell's equations with the given boundary condition, but without entering in the calculations, the interesting solutions belong to two classes:

- **TM modes:** Transverse Magnetic modes, where the axial component of the magnetic field is null
- **TE modes:** Transverse Electric modes, where the axial component of the electric field is null

where every mode has a particular cutoff frequency, and will propagate a wave only in case that the condition  $\omega > \omega_c$  is met (where  $\omega_c = 2\pi f_c$  and  $f_c$  is the cutoff frequency of the mode). The cutoff frequency of each mode depends mainly by the geometry of the guide utilised, and waves with a frequency lower than the cutoff frequency will be exponentially damped.

For particle acceleration purposes, the fundamental feature of a waveguide is that the *phase velocity* is  $v_p = \frac{\omega}{k} > c$ , so it's not suitable for particle synchronous acceleration. That's not surprising and can be understood with simple geometrical considerations[16], furthermore in principle there is no reason to put an upper limit to the phase velocity, since the phase is a geometrical physical quantity. The dispersion relation for a uniform waveguide can be expressed as

$$\omega^2 = \omega_c^2 + (k_0 c)^2 \quad (2.3)$$

where  $\omega_c = K c$  and  $K$  is the cutoff wavenumber.

The *group velocity* instead is  $v_g = \frac{\partial \omega}{\partial k} < c$  as expected for the physical quantity representing the speed of propagation of the EM wave according to Relativity. In any case, waveguides are a key building block of particle accelerators to deliver the RF power from the production equipment to the accelerating cavities.

A particular case is represented by the *Resonant Cavities*, which are closed waveguides at the terminations (e.g. a cylindrical cavity, or *pillbox cavity*, is composed of a circular waveguide closed by two planes at the extremities). In the resonant cavities the EM field can resonate according to the peculiar eigenfrequencies of the system, which are mainly dictated by the geometry. This process allows propagation of just a set of frequencies, just like in the WGs, but when a cavity is operating at one of the eigenfrequency starts to accumulate energy because of the resonance. This mechanism is utilised in accelerating structures.

### 2.1.3 Periodic accelerating structures

Above have been mentioned that the waveguides themselves are not useful to accelerate particles because of the excessive phase velocity. However it's possible to reduce it loading the structure with additional metallic structures, which consists some metallic walls placed orthogonally to the axis of the cavity.

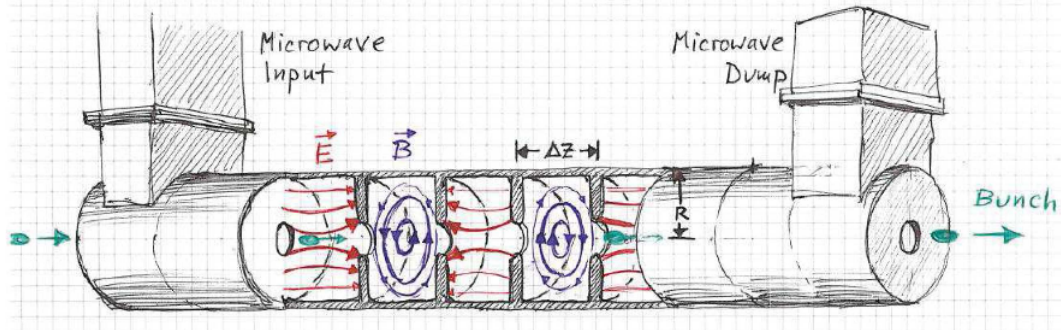


Figure 2.1: Scheme of a travelling wave, disk loaded accelerating structure. In the drawings are visible the input and output couplers, the disk loading the cavity and the beam passing through the irises. From [21]

Such structures are named *Disk (or Iris) Loaded Accelerating Structures*. A schematic example is presented in figure 2.1

The accelerating structure is composed by *cells*, which are connected by the *iris* to the other adjacent cells. At the beginning and the end of the structure are present two special cells that are connected to the input and output coupler for the RF. Apart for the cells with the couplers, the structures present a full rotational symmetry on the beam axis. The role of the irises is creating a free path for the passage of the beam and allowing the propagation of the EM field from the input coupler to the output one. In the case of room temperature cavities the material normally used is Copper, while for superconducting cavities the material can vary and also metallic cavities coated internally with a superconductive layer are a possibility.

From the field perspective, the fact that the accelerating structure is loaded with the disks changes the way that the EM waves propagate in the structure. I won't go through the full mathematical description, which is very detailed in [20, 16], but simply give a general idea of the process and of the relevant results.

The geometry of the accelerating structure can be seen as a cylindrical cavity loaded regularly with the disks. If as first approximation we consider an infinite structure, it is possible to use the *Floquet's Theorem*, that can be summarised as follows: "*In a given mode of an infinite periodic structure, the fields at two different cross sections that are separated by one period differ only by a constant factor, which in general is a complex number*". This has two main implications: there are some regions of the spectrum of  $\omega$  that don't allow the waves to propagate, called *stopbands*, and others, called *passbands*, where the propagation is allowed with a *phase shift*  $\Delta\phi = k_0 d$ , where  $d$  is the length of the cell. The phase advance per cell is a peculiar parameter of every structure, and is defined in the design phase.

The waves that are allowed to propagate in such conditions are called *Space Armonics*, and can be seen as an infinite number of waves propagating at the same frequency but with different wavenumbers. The dispersion relation

becomes

$$\omega^2 = \omega_c^2 + c^2 \left( k_0 + \frac{2\pi n}{d} \right)^2 \quad (2.4)$$

where the principal wave of the mode has  $n = 0$  and the others have  $n$  according to the direction of propagation.

The phase velocity of the  $n$ -th harmonic becomes

$$\beta_n = \frac{\omega}{k_n c} = \frac{\beta_0}{1 + n\beta_0 \lambda/d} \quad (2.5)$$

which allows to reach an arbitrary low phase velocity, as requested for the particle acceleration.

The comparison of the phase velocity of a waveguide and accelerating structure is presented in figure 2.2.

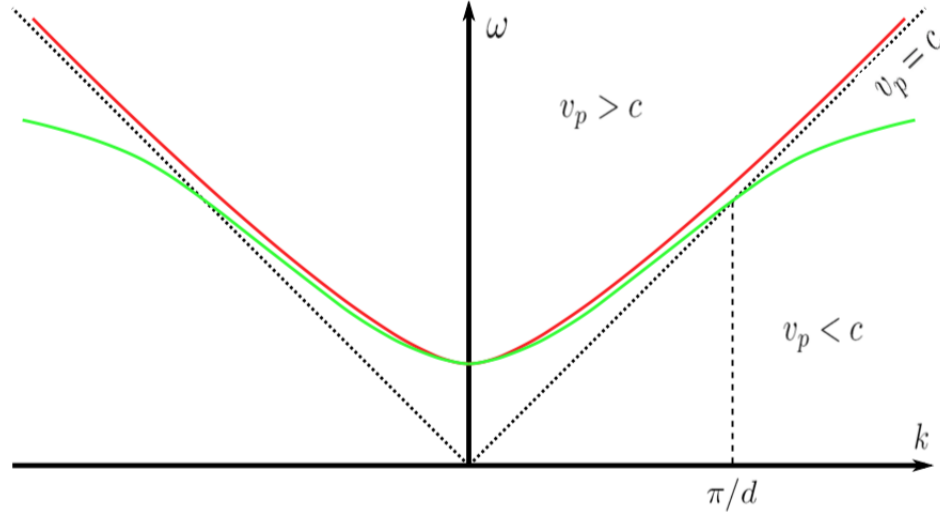


Figure 2.2: Brillouin diagram of a uniform waveguide (red) compared to a disk-loaded accelerating structure (green) [22]

### 2.1.4 Figure of merit for accelerating structures

To characterize the different accelerating structures, is necessary to rely on some significant quantities that can be derived by the geometry of the cavities. The most important figures of merit (FOMs) are the following (many different definitions are commonly used, here are reported in accordance with [23]):

- Quality factor

$$Q_0 = \frac{\omega_0 U}{P_{loss}} \quad (2.6)$$

is a standard FOM for the resonant cavities, representing the stored energy over the power dissipated

- **Shunt impedance**

$$R = \frac{V_{acc}^2}{2P_{loss}} \quad [M\Omega] \quad (2.7)$$

represent the effectiveness of producing an axial voltage  $V_0$  for a given power dissipated. For long cavities, where it is preferable to have a quantity that is independent of the length of the structure, is commonly used the Shunt impedance per unit length

$$Z = \frac{R}{L} \quad [M\Omega/m] \quad (2.8)$$

where  $L$  is the length of the cavity.

- **R over Q**

$$\frac{R}{Q} = \frac{(V_{acc})^2}{2\omega_0 U} \quad [M\Omega] \quad (2.9)$$

represents the relation between the accelerating field and the stored energy

- **Filling time**

$$t_F = \int_0^L \frac{dz}{v_g(z)} \quad (2.10)$$

time needed by the EM field to fill the structure

- **Power delivered to the beam**

$$P_B = \frac{I \Delta W}{q} \quad (2.11)$$

where  $I$  is the beam current and  $\Delta W$  is the energy gain

- **Beam loading ratio**

$$\epsilon_s = \frac{P_B}{P_{tot}} \quad (2.12)$$

represents the fraction of power that is delivered to the beam

## 2.2 High power limits and scaling laws

The limiting factors for room-temperature high-gradient accelerators have been identified as *field emission* and *RF breakdown*. The former is the emission of electrons in the form of the so called "*Dark current*", that subtracts RF power, causes radiation and can produce wakefields; the latter is a limiting factor to the operation of accelerators and can damage the structures.[24]

The understanding of these phenomena is particularly challenging and requires a mixture of notions of disciplines such as surface physics, metallurgy, fabrication processes, microwaves, beam dynamics and plasma physics. At the moment a satisfactory unified theory of the processes that take place during

the breakdowns have not been found yet, then the improvement of the structures is achieved using some scaling laws for the high power limitations, that have been deducted from the experience and the experiments on the structures tested so far.

### 2.2.1 Field emission law

#### Emission from flat clean surface

The field emission law was theorised by Fowler and Nordheim in 1928 and rule the current emission from a metal with applied an intense electric field. The derivation was carried on calculating the tunnel probability of electrons of the conduction band through the perfectly flat and clean surface of a metal.

The applied electric field modify the potential barrier, and the current density of emitted electrons can be derived as the following, giving the *Fowler-Nordheim equation* [25]

$$J_F = \frac{1.54 \times 10^{-6} \times 10^{4.52\phi^{-0.5}} E^2}{\phi} \exp\left(-\frac{6.53 \times 10^9 \phi^{1.5}}{E}\right) \quad [A m^{-2}] \quad (2.13)$$

where  $\phi$  is the work function of the material and  $E$  is the applied electric field.

#### Enhanced field emission

It's well known that almost any surface is never perfectly clean and flat, and also the fact that the asperities of the surface provoke an enhancement of the local electric field. This behaviour lead to the phenomenon known as *Enhanced Field Emission* (EFE), which major contributors are:

- Surface imperfection due to imperfect machining
- Metallic dust
- Molten craters after breakdowns
- Absorbed gas

and some others. These effects can create particular sites known as "emitters". It's a common praxis define the field enhancement factor  $\beta$  to relate the electric field to the microscopic one

$$E_m = \beta E \quad (2.14)$$

and the  $\beta$  factors can be calculated according to the emitter's geometry [26] as exploited in figure 2.3. Once the local field is known, using the formula 2.13 calculate the current emitted from EFE by an emitter site of area A gives

$$I_F = \frac{1.54 \times 10^{-6} \times 10^{4.52\phi^{-0.5}} A \beta^2 E^2}{\phi} \exp\left(-\frac{6.53 \times 10^9 \phi^{1.5}}{\beta E}\right) \quad [A] \quad (2.15)$$

where  $\beta E$  is the local field,  $\phi$  is the work function of the material and  $A$  the area of the considered emitter.

In the RF case the average current emitted is given by similar calculations, averaging the electric field on an RF period [24].

Experimental evidence of the dark current emission have been detected by setups equipped with Faraday Cups, as in [27].

The emission of dark current seems to be a precursor of the breakdown process, even if the relationship between the two processes has not been clarified so far.

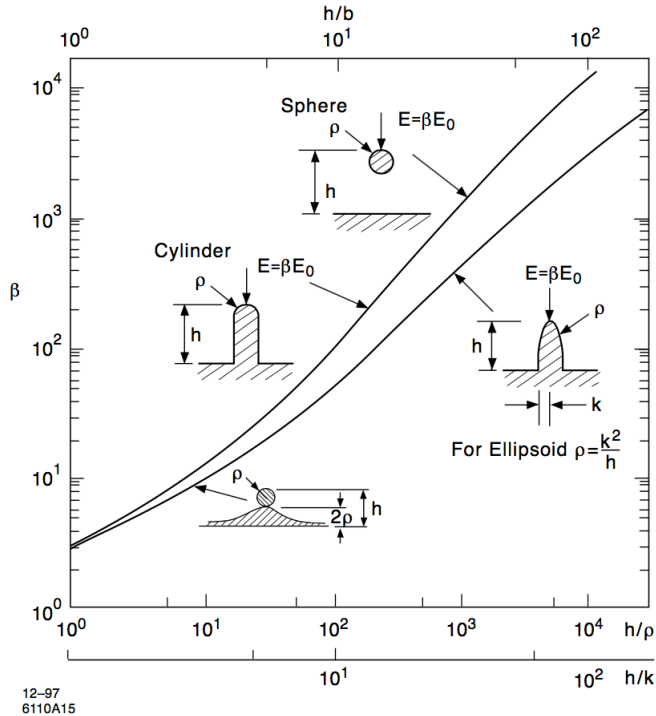


Figure 2.3: Field enhancement factors for simple geometries of metallic protrusions, plotted as function of geometrical features. From [26]

### 2.2.2 Kilpatrick's critereon

The Kilpatrick's Critereon was the first attempt to create a high power limit for the vacuum breakdown valid both in DC and RF applications [28]. The model was based on the acknowledgement of the Field Emission, and suggesting that the vacuum arc was created by the cascade of secondary electrons ejected from the surface by ion bombardment.

Using data collected in the 1950's, the following empirical law was formulated

$$WE^2 \exp(-1.7 \times 10^5 E^{-1}) = 1.8 \times 10^{14} \quad (2.16)$$

where  $W$  is the maximum possible ion energy in eV, and  $E$  is the field in V/m.

This can also be rewritten in the case of the RF to give a frequency limit, as

$$f = 1.64 E^2 \exp\left(-\frac{8.5}{E}\right) \quad (2.17)$$

where  $f$  is the frequency in  $MHz$  and  $E$  is the electric field in  $MV/m$ .

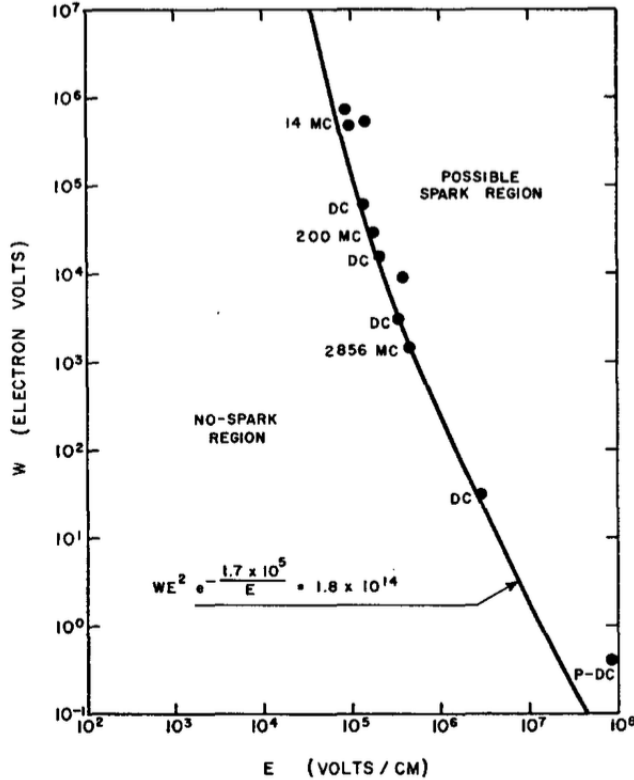


Figure 2.4: Kilpatrick's original plot. Note that  $MC = MHz$  (*Mega Cycles*) and that  $W$  for RF is function of frequency, voltage and gap amplitude. See paper for details [28]

The criteron was reviewed many times up to now, because the experiments conducted nowadays show a limit up to 10 times lower than Kilpatrick's prediction, and this can be addressed to different reasons: first of all the quality of the machining of the structures have increased considerably since the 1950's; in second instance the formula for  $W$  was deducted for parallel plates, but the condition inside the RF cavities are different during operations; and finally the key assumption was that the breakdown was triggered by the secondary emission provoked by the ion bombardment.

At the end of the 1980's J.D.Wang finally proposed a model based on microprotrusion effect on the field and field emission, that involves the formation of a micro-plasma during the breakdown process. Also the Kilpatrick's limit was revised again in order to match the experimental results. [29, 30]

### 2.2.3 Power flow based criteria

Other scalings have been proposed, like the phenomenological  $P/C$ -criterion, where  $P$  is the power flowing in the cavity and  $C$  the minimum iris circumference. It's straightforward to see that this is strongly related to the maximum surface electrical field, which is stronger for smaller irises. Also have to be underlined that this is suitable just to travelling wave structures (TWS), since the power flow in standing wave structures (SWS) is close to zero.

In recent years a more advanced version of the scaling have been presented, which is quantified by

$$\frac{P\tau^{1/3}}{C} \quad (2.18)$$

where  $P$  is the power flow through the structure,  $\tau$  the pulse length and  $C$  the minimum iris circumference. This has also been formulated as  $(f \times P/C)^{0.5}$ , which is a quantity linear with the field [31].

Anyway, although these criteria are still in use today for the accelerating structure design, finding a more general criterion valid for any type of cavity is necessary.

### 2.2.4 The modified Poynting vector $S_c$

During the development of high gradient normal conducting accelerating structures for the CLIC project, was developed a new field quantity, the *Modified Poynting Vector*  $S_c$ , that is suitable both for TWS and SWS. [32]

The founding of this

are that: the breakdown process is a determined by the accumulation of the pulses rather than the single pulse and the possible triggers of the breakdown can be induced by many processes that will be discussed later and are not relevant for the scaling law derivation.

A number of effects have to be taken into account (a simple geometry is considered, a cylindrical protrusion surmounted by a hemispherical cap):

#### Pulsed heating by field emission current

it's known that the field emission gets enhanced by the presence of the protrusion as described before, and in this case the field enhancement factor can be expressed as  $\beta \simeq h/r$ , where  $h$  is the tip height and  $r$  is the cap radius. So the tip will emit a current according to the Fowler-Nordheim law, causing in first approximation the heating of the tip due to the ohmic heating. Assuming that the edge of the tip will be the most heated part, and using the heat conduction equation, it is possible to derive the emitted current to bring the tip to the melted state, which is found to be approximately  $36 A/\mu m^2$  for a tip of  $1 \mu m$  height and a pulse of  $100 ns$ . This is consistent with the findings in [33]. The  $\beta$  factor can be then derived, which is approximately between 40 and 60 considering a surface electric field in case of breakdown between 200 and 300  $MV/m$ .

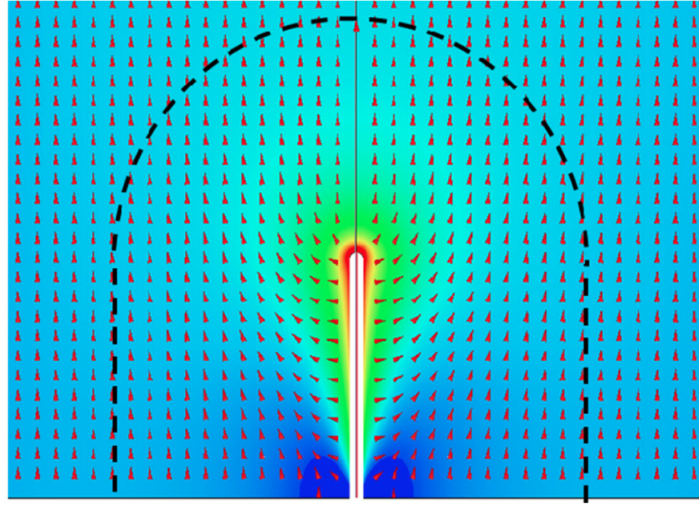


Figure 2.5: Electric field distribution around the protrusion considered. Arrows indicate the direction of the field and the color code the absolute value of the field, mapped logarithmically [32]

### Power flow near an emission site

The heating of the tip mentioned before requires a huge amount of energy, which can be supplied only by the RF power present into the cavity. This is described by the Poynting vector  $S_{RF} = E \times H_{RF}$ . As discussed before a current is established in the tip, and flows through, subtracting energy to the EM field in the surroundings of the tip; the current flows through the tip and leave it at the edge, getting sprayed in the cavity according to the Fowler-Nordheim theory. Since any current flowing creates an associated magnetic field, the power flow due to the emission is given by  $S_{FN} = E \times H_{FN}$ .

The key point is that since the copper is a very good conductor, so to provoke a notable ohmic heating of the tip, a significant power flow through the tip is necessary. This can be calculated evaluating the  $S_{FN}$  at a distance  $d = h$  from the edge of the tip, where the electric field is not perturbed anymore by the shape of the tip itself. This can be formulated as the condition

$$P_{RF} \geq P_{FN} \gg P_{loss} \quad (2.19)$$

where  $P_{loss}$  is the power lost for ohmic heating and  $P_{FN}$  the power flow through the tip.

Considering now the relative phase of the  $P_{RF}$  and of the  $P_{FN}$  it is possible to derive an expression for the power emitted in a copper cavity

$$P_{FN}(t) = A E_0^3 \sin^3 \omega t \exp\left(\frac{-62}{\beta E_0 \sin \omega t}\right) \quad (2.20)$$

where the work function for the copper have been used is  $\phi = 4.5 \text{ eV}$ ,  $A$  is the area of the conductor and  $\omega = 2\pi f$  is the angular velocity.

The RF power can be divided in real and imaginary part, with a phase shift of  $90^\circ$ . The real part is the energy propagating into the structure only and the imaginary part is the energy stored in the cavity both magnetically or electrically as happens in every resonant cavity. Since the active power flow is more efficient than the reactive one in providing power for the field emission, a weighting factor  $g_c$  is introduced. Also for practice reasons since all the simulation codes work using the complex Poynting vector  $\bar{S}$ , the precedent reasoning can be adapted to meet the custom, using the *Modified Poynting Vector*

$$S_c = \text{Re}\{\bar{S}\} + g_c \text{Im}\{\bar{S}\} \quad [W/\mu m^2] \quad (2.21)$$

Since this quantity can be calculated in any point of a structure, this allows to identify in advance the regions which are more sensible to the breakdown process. The rule of thumb given by the current experience says that this quantity should not exceed the value of  $5W/\mu m^2$  to have a breakdown rate smaller than  $1 \times 10^{-6} \text{ bpp m}^{-1}$  with a pulse length of 200 ns.

This quantity have been used successfully to design all the last generations of CLIC structures, including the one tested in this work.

## 2.3 The TD26CC structure for the Main Beam of CLIC

After the precedent part about the general laws that regulate the operation of the TWS, now will be presented the structure under test in this work, the TD26CC, which stays for Tapered, Damped, 26-cells active cells structure with Compact Couplers.

It's necessary to keep present in mind that in the design of the real cavities, it's almost never possible to use the general laws described in precedence because of the high complexity of the geometries. A great work of design and simulation is necessary then, and is carried out with complex numerical simulations. In this section will be presented a summary of the parameters and features of the cavity, the details can be found in [9, 34, 35].

As pointed out in [9], the main constraints in the structures for the main beam LINAC are

1. Maximum surface electric field:  $E_{\text{surf}}^{\max} < 260 \text{ MV/m}$
2. Pulsed surface heating:  $\Delta T^{\max} < 56 \text{ K}$
3. Power density:  $P_{\text{in}}/C\tau_p^{1/3} < 18 \text{ MW/mm ns}^{1/3}$

where  $P_{\text{in}}$  is the input power,  $C$  is the input iris circumference and  $\tau_p$  is the pulse length.

These limitations, together with the parameters listed in the section 1.2.2, brought to the current design after a long simulation and tradeoff of the parameters. The main parameters are reported in Table 2.1

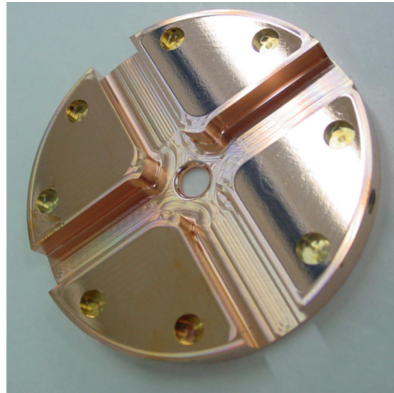
Average loaded accelerating gradient	$100 \text{ MV/m}$
Frequency	$12 \text{ GHz}$
RF phase advance per cell	$2/3\pi \text{ rad}$
Average iris radius to wavelength ratio	0.11
Input, output iris radii	$3.15, 2.35 \text{ mm}$
Input, output iris thickness	$1.67, 1.00 \text{ mm}$
Input, output group velocity	$1.65, 0.83 \% \text{ of } c$
First, last cell Q-factor	5536, 5738
First, last cell shunt impedance	$81, 103 \text{ M}\Omega/\text{m}$
Number of regular cells	26
Structure length including couplers	$230 \text{ mm}$
Filling time	$67 \text{ ns}$
Total pulse length	$242 \text{ ns}$
Peak input power	$61.3 \text{ MW}$
RF-to-beam efficiency	27.7%
Maximum surface electric field	$230 \text{ MV/m}$
Maximum pulsed surface heating	$47 \text{ K}$

Table 2.1: Parameters of the structure

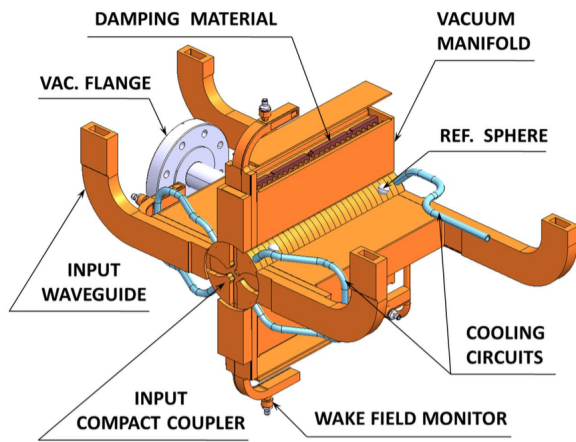
The structure is realised stacking machined copper disks that are then brazed together with a particular procedure that have been elaborated in order to achieve the highest mechanical precision possible in the alignment of the parts. In figure 2.6 are shown a disk and a model of the accelerating structure. Please note that the only difference between the model in the figure and the prototype under test is the absence of the wakefield monitor in the prototype.

Because of the high number of bunches per train and of the short spacing between them, the structure is realised in order to extract the transverse wakefields that can develop in the structure. This is realised using 4 symmetrical waveguides of dimensions carefully selected in order to extract just the higher order electromagnetic modes (HOMs) but not the fundamental one that is used to accelerate the bunches and is provided from the input couplers. Once extracted, the transverse wakefields are dumped on tips of Silicon Carbide (SiC) that are placed at 50 mm of distance from the axis of the cavity.

The iris radius and thickness are linearly tapered in order to optimise the various high power parameters and avoid the presence of 'hot spots' along the structure. The tapering also provide detuning of the high order modes, which are an issue even for highly damped structures.



(a) A disk composing the structure



(b) CAD model of the structure, open to show the damping material

Figure 2.6: A disk composing the structure (left) and the scheme of an accelerating structure (right), including couplers for the RF, cooling elements and connection flanges

# Chapter 3

## The breakdown process

3.1 phase1

3.2 phase2

3.3 phase3

Enumeration example

# Chapter 4

## Experimental setup

### 4.1 The TD26 accelerating structure

### 4.2 The LINAC and the Dogleg

Bullet list example

- first point
- second point
- third point

### 4.3 RF power generation

Enumeration example

1. first point
2. second point
3. third point

Description example

**first descr** first point

**second descr** second point

**third descr** third point

## 4.4 DAQ system

### 4.4.1 Hardware

### 4.4.2 Online triggers

describe the online, but then the offline is in the next chapter  
... but you can also build nested lists

- first point
  - first point
  - second point
- second point
- third point

## 4.5 Other systems

mention here thermal systems for the structure and something else ???

# Chapter 5

## Data analysis tools

### 5.1 Offline selection of the events

A tabular example

Tit1	Tit2
el1	el2
el1	el2
el1	el2

but tabulars cannot be captioned ! (are in text elements)

Using the table environment, the caption works ! BUT BECOMES FLOATING OBJECTS (in fact is on the bottom of the page due to no more text inserted afterwards).

Same thing for the figure environment

### 5.2 Time and space positioning of the breakdowns

### 5.3 Migration of the breakdowns

### 5.4 Beam induced RF

### 5.5 Neural network based events selection

1	2	3
4	5	6
7	8	9

Table 5.1: A simple table

# Chapter 6

## Results and future developments

### 6.1 Results

A figure example, with text in line (NO CAPTION)



A figure example, with floating object and caption

### 6.2 Further developments



Figure 6.1: the logo of UniTo

# List of abbreviations

BSM	Beyond Standard Model
CDR	Conceptual Design Report
CERN	Conseil européen pour la Recherche nucléaire, Geneva, Switzerland
CLIC	Compact Linear Collider
CTF3	CLIC test facility 3
EFE	Enhanced Field Emission
EM	Electromagnetism -or- electromagnetic
FCC-ee	Future Circular Collider, lepton version
FCC-hh	Future Circular Collider, hadron version
FOM	Figure Of Merit
HOM	High(er) Order Mode
ICFA	International Committee for Future Accelerators
ILC	International Linear Collider
KEK	High Energy Accelerator Research Organization, Tsukuba, Japan
LEP	Large Electron Positron Collider
LHC	Large Hadron Collider
LINAC	Linear Accelerator
NC	Normal Conducting
PETS	Power Extraction and Transfer Structure
RF	Radio frequency
SC	Super Conducting
SLAC	Stanford Linear Accelerator, Menlo Park, California
SM	Standard Model
SPS	Super Proton Synchrotron
SWS	Standing Wave Structure
TBM	Two-Beams module
TDR	Technical Design Report
TE	Transverse Electric (modes of a WG)
TM	Transverse Magnetic (modes of a WG)
TWS	Travelling Wave Structure
WG	Waveguide
XBOX	X-band high power RF test stand

# List of Figures

1.1	Layout of the final stage of CLIC	6
1.2	Design of a Two-beam module.	6
1.3	Map of the CLIC facility, if implemented in the Geneva area .	7
2.1	Scheme of a travelling wave, disk loaded accelerating structure. In the drawings are visible the input and output couplers, the disk loading the cavity and the beam passing through the irises. From [21]	12
2.2	Brillouin diagram of a uniform waveguide (red) compared to a disk-loaded accelerating structure (green) [22]	13
2.3	Field enhancement factors for simple geometries of metallic pro- trusions, plotted as function of geometrical features. From [26] .	16
2.4	Kilpatrick's original plot. Note that $MC = MHz$ ( <i>Mega Cycles</i> ) and that $W$ for RF is function of frequency, voltage and gap amplitude. See paper for details [28]	17
2.5	Electric field distribution around the protrusion considered. Ar- rows indicate the direction of the field and the color code the absolute value of the field, mapped logarithmically [32]	19
2.6	A disk composing the structure (left) and the scheme of an accelerating structure (right), including couplers for the RF, cooling elements and connection flanges .	22
6.1	the logo of UniTo	27

# List of Tables

1.1	Comparison of two circular machines, LEP[7] and FCC-ee[7, 8] and the two projects for linear machines, the first and last stage of the CLIC implementation [9] and the final stage of ILC[10]	4
1.2	CLIC main parameters in the final stage	8
2.1	Parameters of the structure	21
5.1	A simple table	26

# Bibliography

- [1] S. Chatrchyan *et al.*, “Observation of a new boson at a mass of 125 GeV with the CMS experiment at the LHC,” *Phys. Lett.*, vol. B716, pp. 30–61, 2012.
- [2] G. Aad *et al.*, “Observation of a new particle in the search for the Standard Model Higgs boson with the ATLAS detector at the LHC,” *Phys. Lett.*, vol. B716, pp. 1–29, 2012.
- [3] O. S. Bruening, P. Collier, P. Lebrun, S. Myers, R. Ostojic, J. Poole, and P. Proudlock, *LHC Design Report*. Geneva: CERN, 2004.
- [4] “Icfa statement on linear colliders.” [http://icfa.fnal.gov/statements/icfa\\_lcstatement/](http://icfa.fnal.gov/statements/icfa_lcstatement/).
- [5] A. D. Martin, W. J. Stirling, R. S. Thorne, and G. Watt, “Parton distributions for the lhc,” *The European Physical Journal C*, vol. 63, no. 2, pp. 189–285, 2009.
- [6] J. R. Ellis and I. H. Wilson, “New physics with the compact linear colider,” *Nature*, vol. 409, pp. 431–435, 2001.
- [7] J. W. et al., “Future Circular Collider Study - Lepton Collider Parameters,” Tech. Rep. FCC-1401201640-DSC, CERN, Geneva, Jun 2016.
- [8] F. Zimmermann, M. Benedikt, K. Oide, A. Bogomyagkov, E. Levichev, M. Migliorati, and U. Wienands, “Status and Challenges for FCC-ee,” Tech. Rep. CERN-ACC-2015-0111, CERN, Geneva, Aug 2015.
- [9] M. Aicheler, P. Burrows, M. Draper, T. Garvey, P. Lebrun, K. Peach, N. Phinney, H. Schmickler, D. Schulte, and N. Toge, “A Multi-TeV Linear Collider Based on CLIC Technology: CLIC Conceptual Design Report,” Tech. Rep. CERN-2012-007. SLAC-R-985. KEK-Report-2012-1. PSI-12-01. JAI-2012-001, Geneva, 2012.
- [10] T. Behnke, J. E. Brau, B. Foster, J. Fuster, M. Harrison, J. M. Patterson, M. Peskin, M. Stanitzki, N. Walker, and H. Yamamoto, “The International Linear Collider - Volume 1: Executive Summary,” Tech. Rep. CERN-ATS-2013-037. ILC-REPORT-2013-040. KEK-Report-2013-1., Geneva, Jun 2013.

## BIBLIOGRAPHY

---

- [11] R. Corsini, “Experimental verification of the CLIC two-beam scheme, status and outlook,” *Conf. Proc.*, vol. C1205201, p. TUOBC01. 3 p, May 2012.
- [12] P. Lebrun, L. Linssen, A. Lucaci-Timoce, D. Schulte, F. Simon, S. Staines, N. Toge, H. Weerts, and J. Wells, “The CLIC Programme: Towards a Staged  $e^+e^-$  Linear Collider Exploring the Terascale: CLIC Conceptual Design Report,” Tech. Rep. CERN-2012-005, Geneva, 2012.
- [13] M. J. Boland, U. Felzmann, P. J. Giansiracusa, T. G. Lucas, R. P. Rassool, C. Balazs, T. K. Charles, K. Afanaciev, I. Emeliantchik, and Ignatenko, “Updated baseline for a staged Compact Linear Collider,” Tech. Rep. arXiv:1608.07537. CERN-2016-004, Geneva, Aug 2016.
- [14] I. Bozovic-Jelisavcic, “CLIC Physics Overview,” Tech. Rep. CLICdp-Conf-2016-006, CERN, Geneva, Jun 2016.
- [15] P. G. Roloff, “Higgs Physics at the CLIC Electron-Positron Linear Collider,” Tech. Rep. CLICdp-Pub-2016-001, CERN, Geneva, Aug 2016.
- [16] M. Weiss, “Introduction to rf linear accelerators,” *CAS - CERN Accelerator school: 5th General accelerator physics course*, 1994.
- [17] T. P. Wangler, *RF linear accelerators; 2nd rev. version.* Physics textbook, Weinheim: Wiley, 2008.
- [18] S. Humphries, *Principles of charged particle acceleration.* New York, NY: Wiley, 1986.
- [19] E. Botta and T. Bressani, *Elementi di elettromagnetismo avanzato.* Aracne editrice, 1 ed., Jan 2009.
- [20] J. D. Jackson, *Classical electrodynamics; 2nd ed.* New York, NY: Wiley, 1975.
- [21] A. Streun, “Experimental methods of particle physics - particle accelerators. lecture slides.” <https://ados.web.psi.ch/empp-streun/empp.pdf>. Last accessed 4 Feb 2017.
- [22] J. W. Kovermann, A. Stahl, and W. Wuensch, *Comparative Studies of High-Gradient Rf and Dc Breakdowns.* PhD thesis, Aachen, Tech. Hochsch., Aachen, 2010. Presented 17 Dec 2010.
- [23] F. Tecker, “RF Systems,” *CAS - CERN Accelerator school: Introduction to Accelerator Physics 2016*, Oct 2016.
- [24] J. W. Wang and G. A. Loew, “Field emission and RF breakdown in high gradient room temperature linac structures,” in *Frontiers of accelerator technology. Proceedings, Joint US-CERN-Japan International School, Hayama and Tsukuba, Japan, September 9-18, 1996*, pp. 768–794, 1997.

## BIBLIOGRAPHY

---

- [25] R. H. Fowler and L. Nordheim, “Electron emission in intense electric fields,” *Proceedings of the Royal Society of London A: Mathematical, Physical and Engineering Sciences*, vol. 119, no. 781, pp. 173–181, 1928.
- [26] F. Rohrbach, *CERN 71-28*. Geneva, 1971.
- [27] W. Wuensch, “Advances in the Understanding of the Physical Processes of Vacuum Breakdown,” Tech. Rep. CERN-OPEN-2014-028. CLIC-Note-1025, CERN, Geneva, May 2013.
- [28] W. D. Kilpatrick, “Criterion for vacuum sparking designed to include both rf and dc,” *Review of Scientific Instruments*, vol. 28, no. 10, pp. 824–826, 1957.
- [29] J. W. Wang, “SOME PROBLEMS ON RF BREAKDOWN IN ROOM TEMPERATURE ACCELERATOR STRUCTURE: A POSSIBLE CRITERION,” 1986.
- [30] A. S. Verdu, “Kilpatrick’s critereon, an historical perspective.” [http://indico.cern.ch/event/76081/contributions/2086273/attachments/1051717/1499553/Kilpatricks\\_Criterion.pdf](http://indico.cern.ch/event/76081/contributions/2086273/attachments/1051717/1499553/Kilpatricks_Criterion.pdf), December 2009. Last accessed 31 Jan 2017.
- [31] W. Wuensch, “Observations about RF Breakdown from the CLIC High Gradient Testing Program,” Dec 2006. revised version submitted on 2006-12-12 10:52:40.
- [32] A. Grudiev, S. Calatroni, and W. Wuensch, “New local field quantity describing the high gradient limit of accelerating structures,” *Phys. Rev. Spec. Top. Accel. Beams*, vol. 12, p. 102001, 2009.
- [33] E. A. Litvinov, G. A. Mesyats, and D. I. Proskurovskii, “Field emission and explosive electron emission processes in vacuum discharges,” *Soviet Physics Uspekhi*, vol. 26, no. 2, p. 138, 1983.
- [34] A. Grudiev and W. Wuensch, “Design of the Clic main Linac accelerating structure for Clic conceptual design report,” p. 3 p, Sep 2010.
- [35] A. Lunin, V. Yakovlev, and A. Grudiev, “Analytical solutions for transient and steady state beam loading in arbitrary traveling wave accelerating structures,” *Phys. Rev. Spec. Top. Accel. Beams*, vol. 14, p. 052001. 11 p, Dec 2010.